Electronic Supplementary Material (ESI) for Nanoscale.

Supporting Information for "Digestion of lipid micelles leads to increased membrane permeability"

Jun Xie,[†] Demi L. Pink,[†] M.Jayne Lawrence,[‡] and Christian D. Lorenz*,[†]

†*Department of Physics, King's College London, London*

‡*Division of Pharmacy Optometry, University of Manchester, Manchester*

E-mail: chris.lorenz@kcl.ac.uk

Phone: +44 (0)2078482639

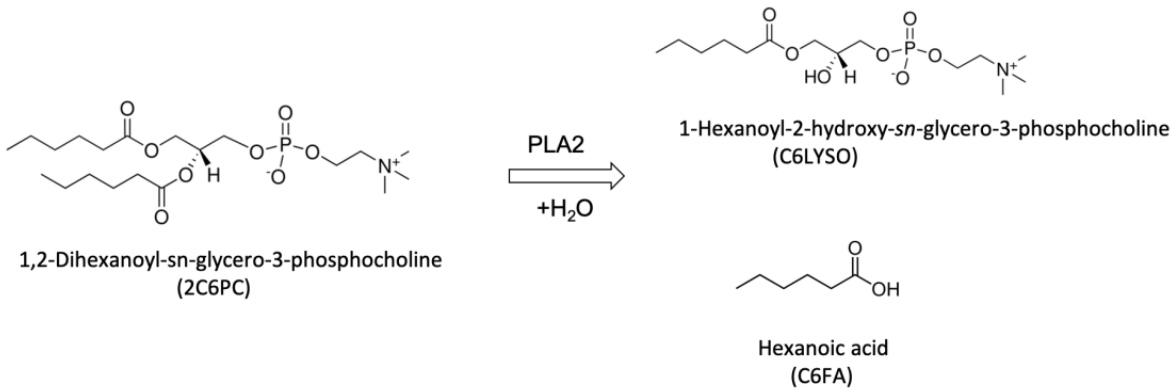

Figure S1: The chemical structure of three species. The parent 2C6PC molecules are degraded via hydrolysis alongside the C6FA and C6LYSO product molecules.

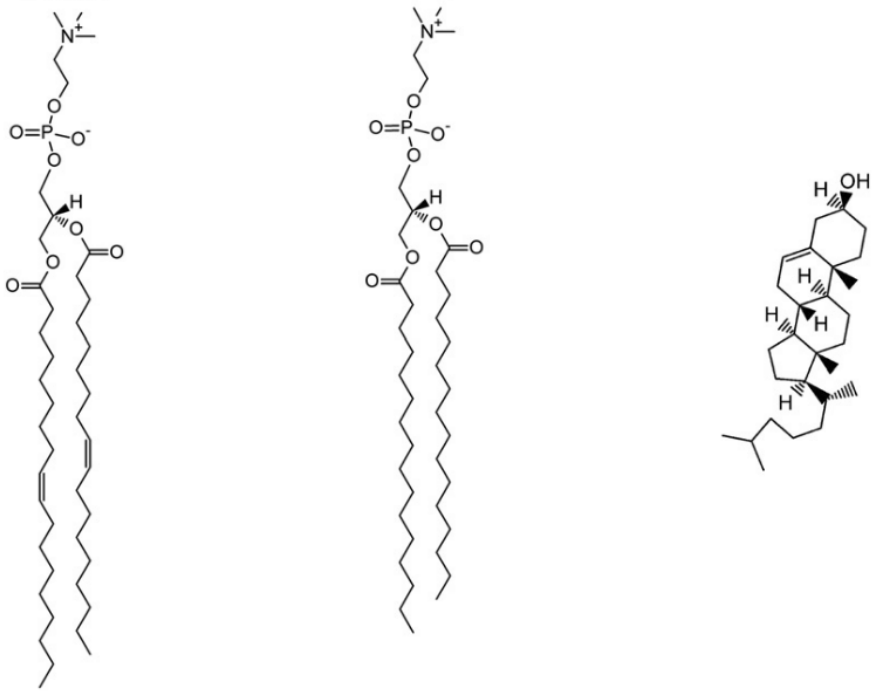

Figure S2: Chemical structures of DOPC, DPPC and cholesterol respectively.

Table S1: Detailed Description of the Composition of All of the Eight Simulated Systems.

System abbreviation	DOPC	DPPC	CHOL	C6PC	C6FA	C6LYSO	Na+	Cl-	water	MD length (ns)
DOPC	350	0	0	0	0	0	47	47	16824	200
DPPC-CHOL	0	308	132	0	0	0	43	43	15900	200
DOPC-Pure-Products	350	0	0	0	29	21	111	111	40870	1000
DOPC-Mixed	350	0	0	16	16	12	110	110	39850	1200
DOPC-Pure-Lipids	350	0	0	35	0	0	111	111	40901	1400
DPPC-CHOL-Pure-Products	0	308	132	0	29	21	58	58	21465	1000
DPPC-CHOL-Mixed	0	308	132	16	16	12	59	59	21553	1000
DPPC-CHOL-Pure-Lipids	0	308	132	35	0	0	57	57	20939	1000

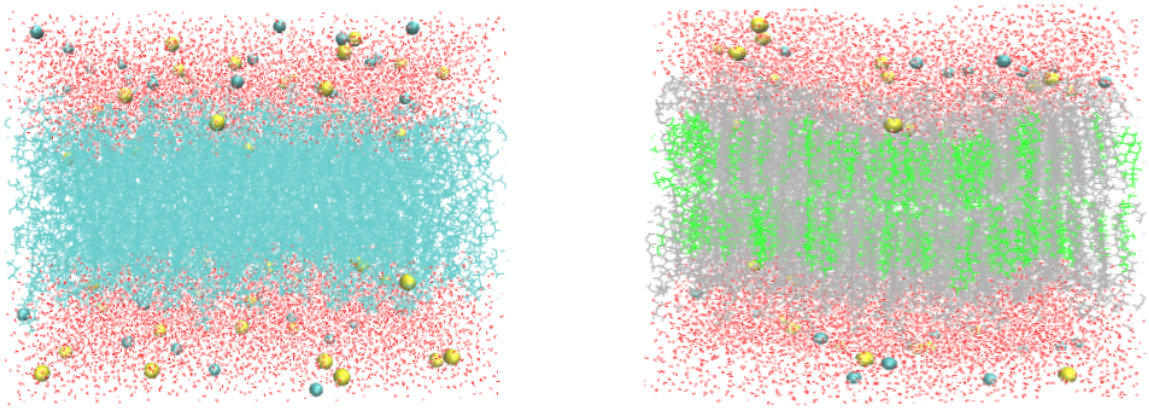

Figure S3: Snapshots of two membranes in the 200 ns time frames of trajectory. Left is the DOPC only system with ions, where Na+ is yellow, Cl- is blue, water is in red and DOPC is located in the middle of the box. Right is DPPC-CHOL membrane, where DPPC shown in grey and cholesterol in green respectively.

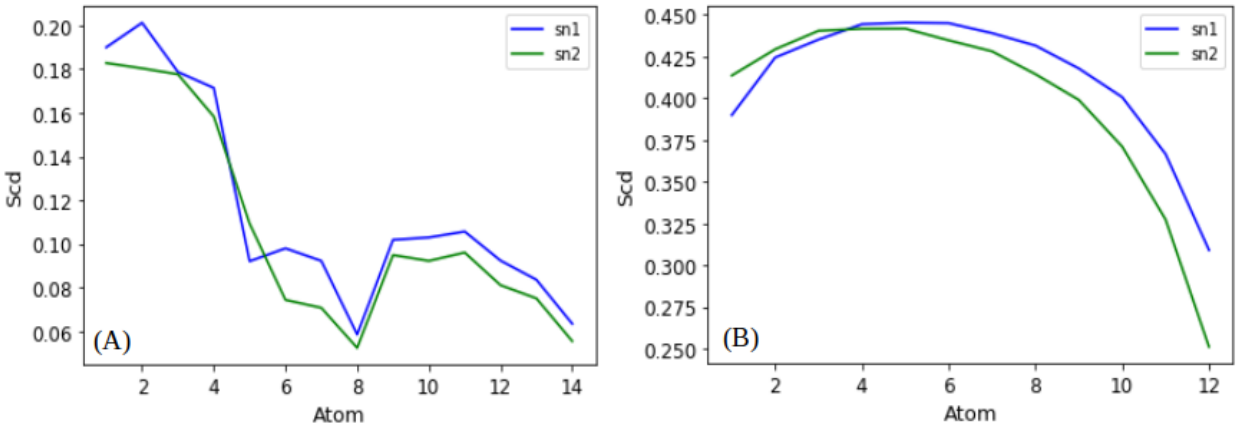

Figure S4: Absolute values of order parameters, S_{cd} , as a function of carbon number for the (A) DOPC and (B) DPPC-CHOL membrane systems interacting with micelles.

Table S2: The summary of each molecules' mean tilt angle, and the standard errors are shown in parentheses. The tilt angle reported for C6PC, DOPC and DPPC are calculated by measuring the cosine of the angle formed by the vector defined by the P and N atoms in their PC headgroups (Figs. S1 and S2) and the normal to the membrane; while the tilt angle of C6FA is calculated by measuring the cosine of the angle formed by the vector connecting the C2 and O2 atoms of the molecule (see Fig. S8) and the the normal vector of the membrane.

System	DOPC-Pure-Products	DOPC-Mixed	DOPC-Pure-Lipids	DPPC-CHOL-Pure-Products	DPPC-CHOL-Mixed	DPPC-CHOL-Pure-Lipids
C6FA	0.644 (0.008)	0.635 (0.006)	-	0.681 (0.003)	-	-
C6PC	-	0.327 (0.007)	0.301 (0.004)	-	-	-
DOPC	0.338 (0.003)	0.344 (0.002)	0.344 (0.001)	-	-	-
DPPC	-	-	-	0.341 (0.002)	0.343 (0.004)	0.391 (0.002)

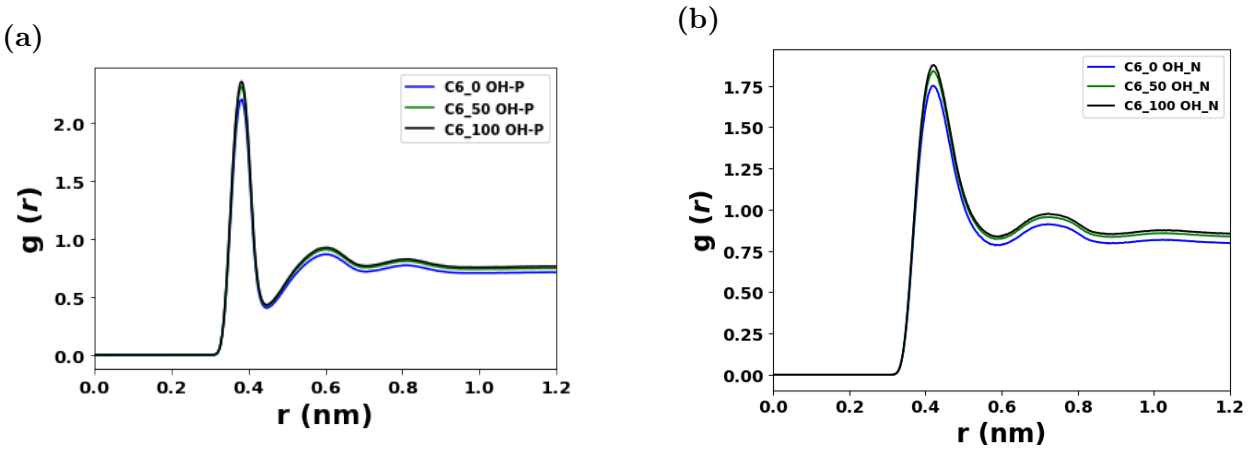

Figure S5: Radial distribution function ($g(r)$) of O_W around (a) the P and (b) N atoms in the PC head groups in the three DOPC membrane systems (Pure-Products (blue) , Mixed (green), Pure-Lipids (black)).

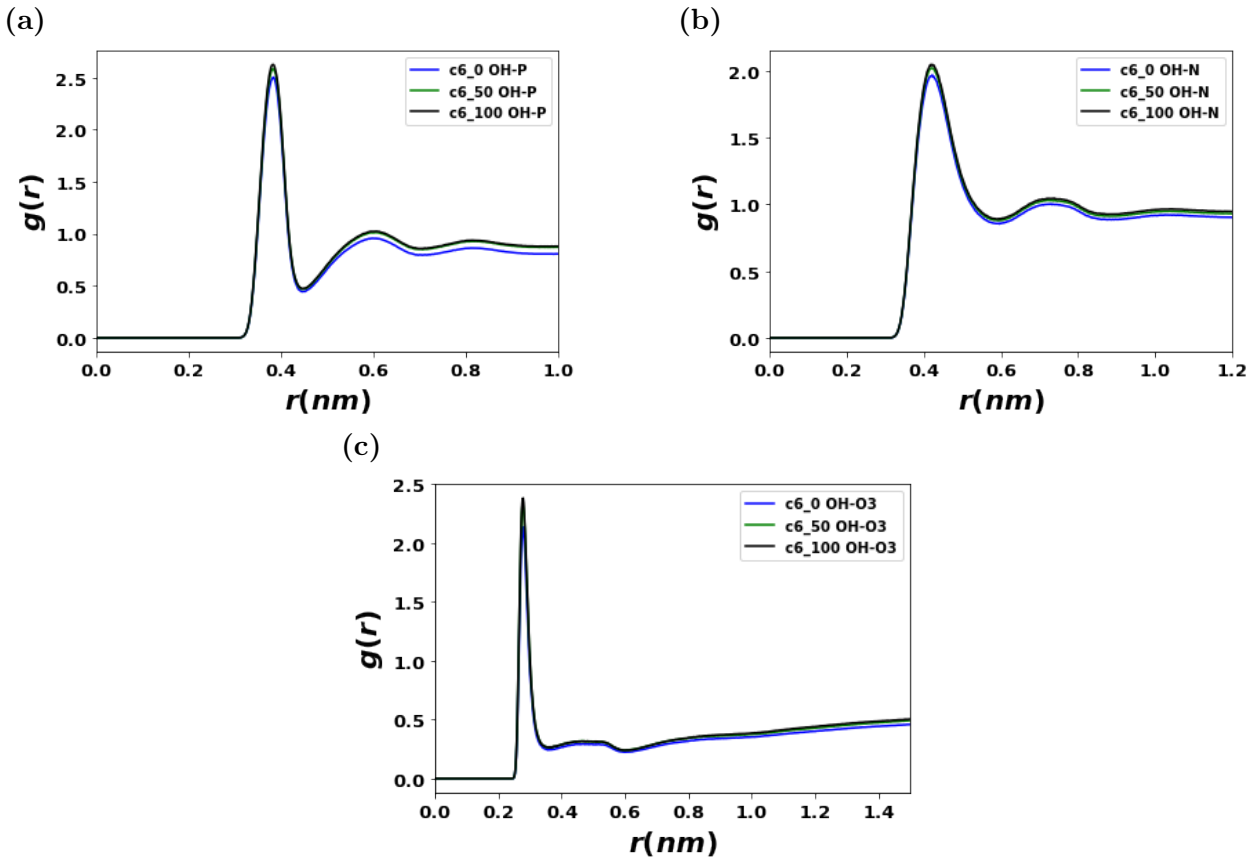

Figure S6: Radial distribution function ($g(r)$) of O_W around (a) the P and (b) N atoms in the PC head groups and (c) the O3 atom in the C6FA molecules (see Fig. S8) in the three DPPC-CHOL membrane systems (Pure-Products (blue) , Mixed (green), Pure-Lipids (black))

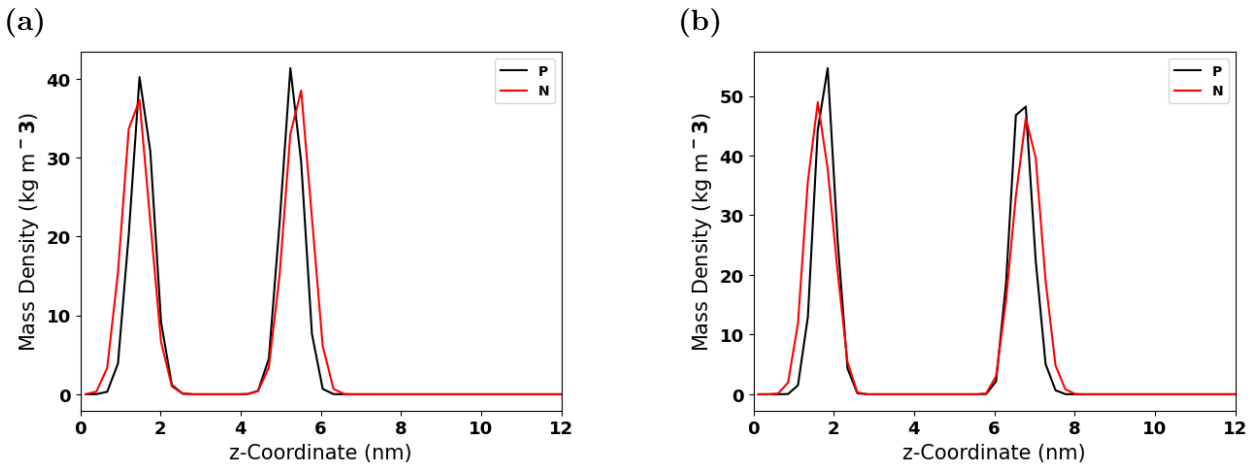

Figure S7: Mass density profiles of atom P and N in DOPC (a) or DPPC-CHOL (b) mixed membrane systems.

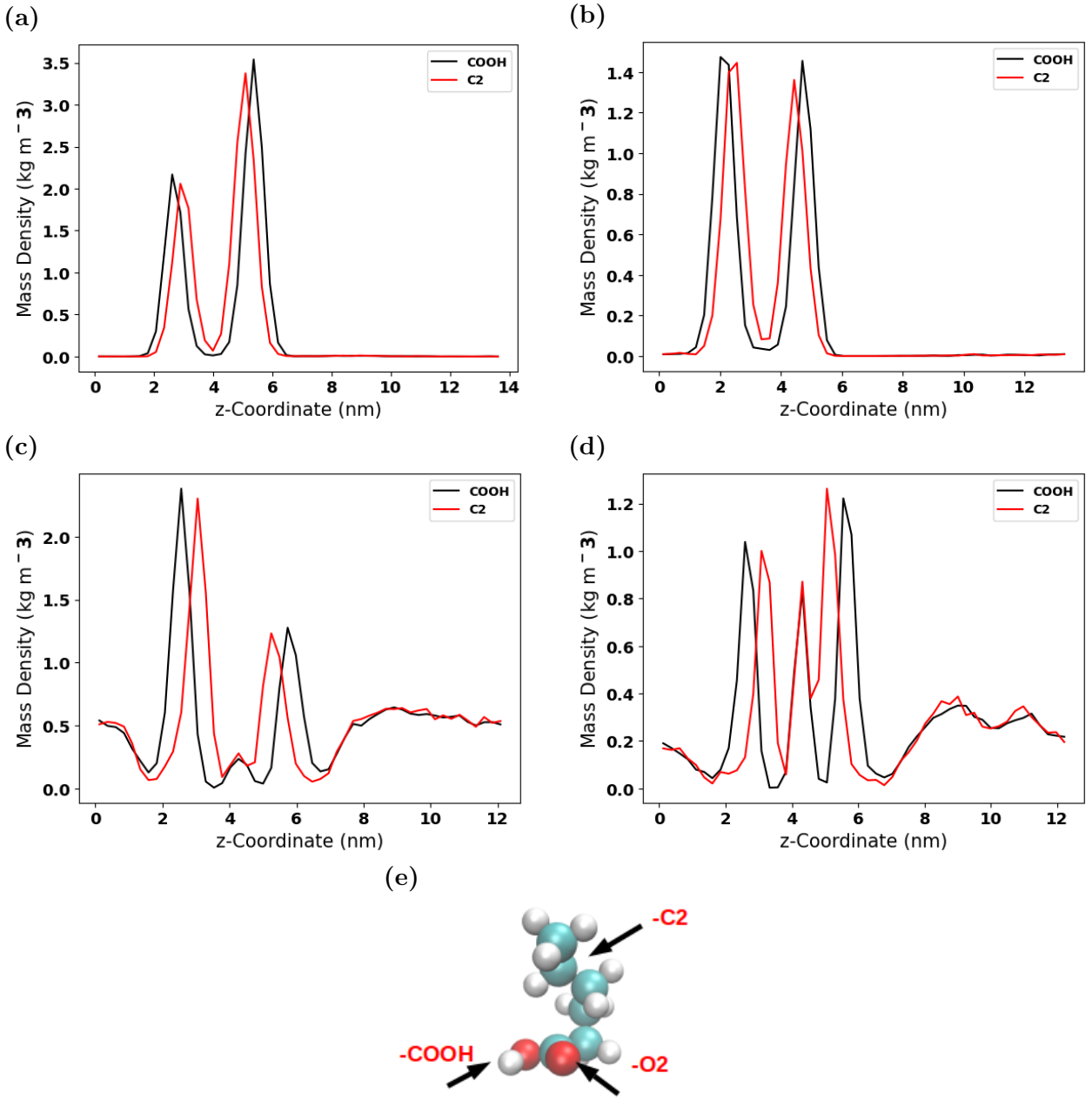

Figure S8: Mass density profiles of -COOH and C2 for C6FA in DOPC membrane systems with micelles (a) Pure-Products, (b) Mixed and DPPC-CHOL membrane systems with micelles (c) Pure-Products, (d) Mixed, (e) the structure of C6FA and atom labels that used for measuring the orientations of C6FA

Table S3: The first coordinate shell (nm) for the water oxygen atoms O_W with P, N, O3 from headgroups, glycerol ester and cholesterol respectively. The coordination number of waters is shown in parentheses.

System	Pure-DOPC	DOPC-Pure-Products	DOPC-Mixed	DOPC-Pure-Lipids	Pure-DPPC-CHOL	DPPC-CHO-Pure-Products	DPPC-CHOL-Mixed	DPPC-CHOL-Pure-Lipids
P	0.448(6.4)	0.448(6.4)	0.448(6.3)	0.448(6.3)	0.443(0.59)	0.446(5.9)	0.444(6.0)	0.446(6.0)
N	0.459(18.4)	0.604(19.4)	0.582(17.5)	0.584(17.6)	0.589(17.4)	0.596(17.4)	0.590(16.9)	0.594(17.1)
CHOL-O3	-	-	-	-	0.357(2.0)	0.358(2.0)	0.362(2.0)	0.368(2.1)

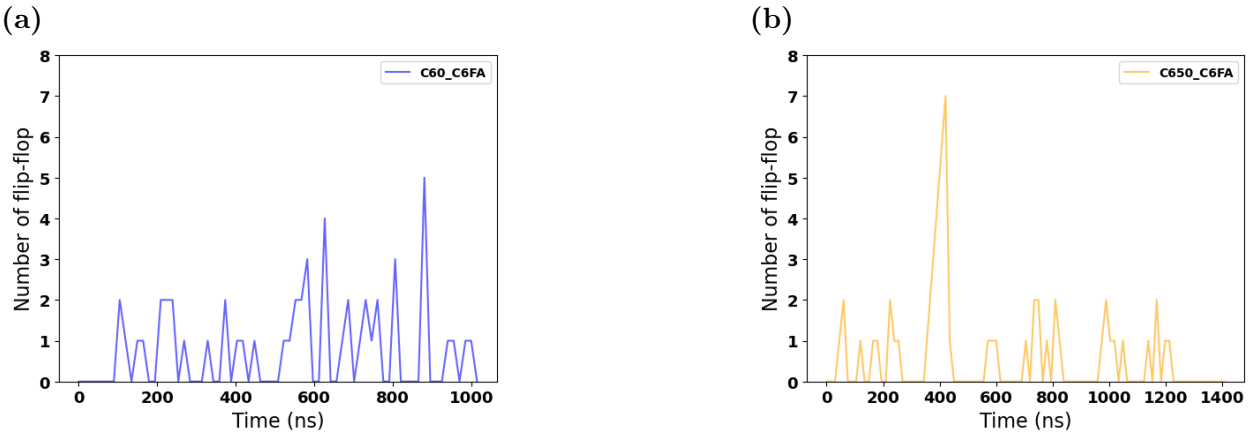

Figure S9: Number of flip-flip event for C6FA in DOPC-Pure-Products (a) and DOPC-Mixed (b) systems over time.

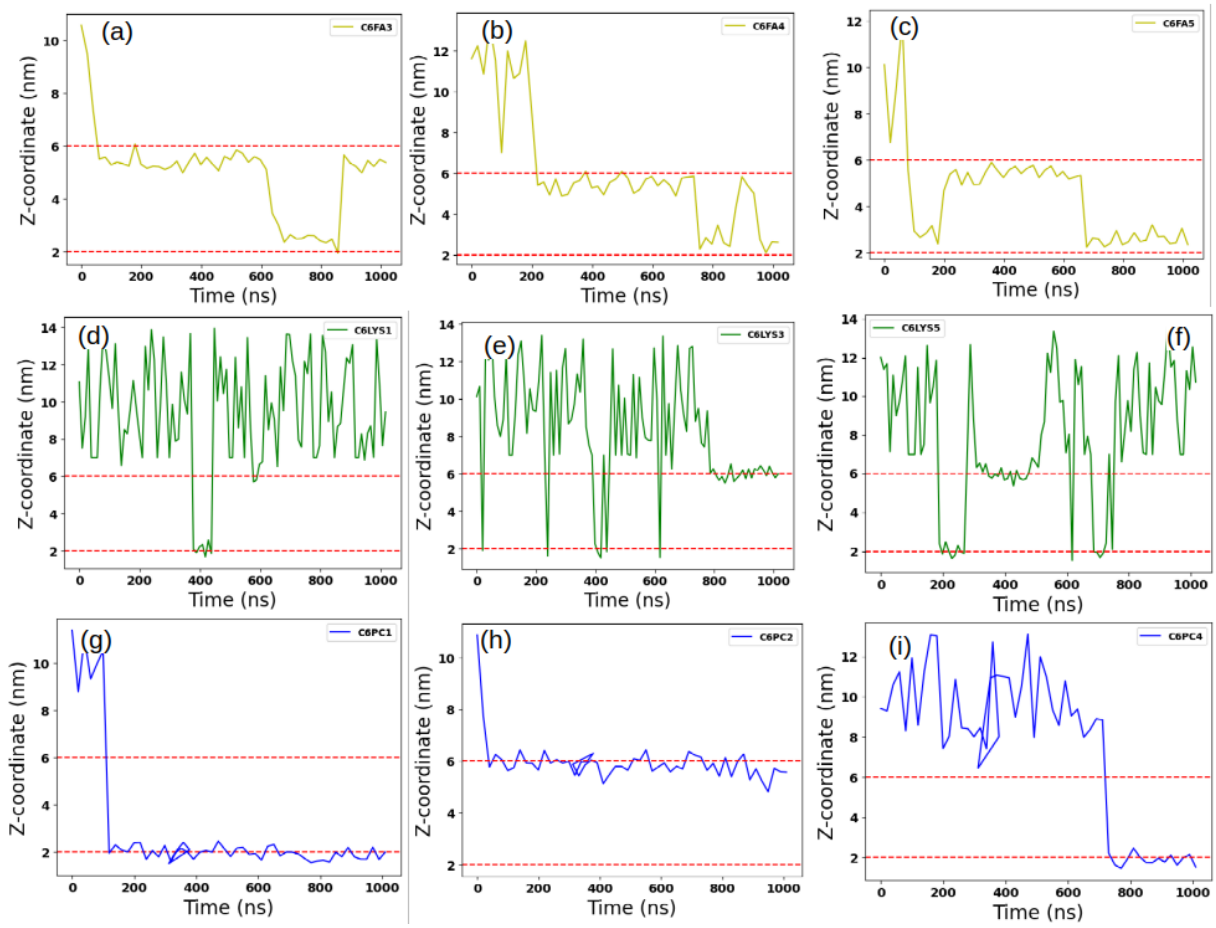

Figure S10: Z-coordinate of different molecules in DOPC membrane system profiles over time (a-c)C6FA, (d-f) C6LYS, (h-i) C6PC and the number followed after the molecule names indicate the index for different molecules. The red dashed lines represent the upper and lower limits of the bilayers.

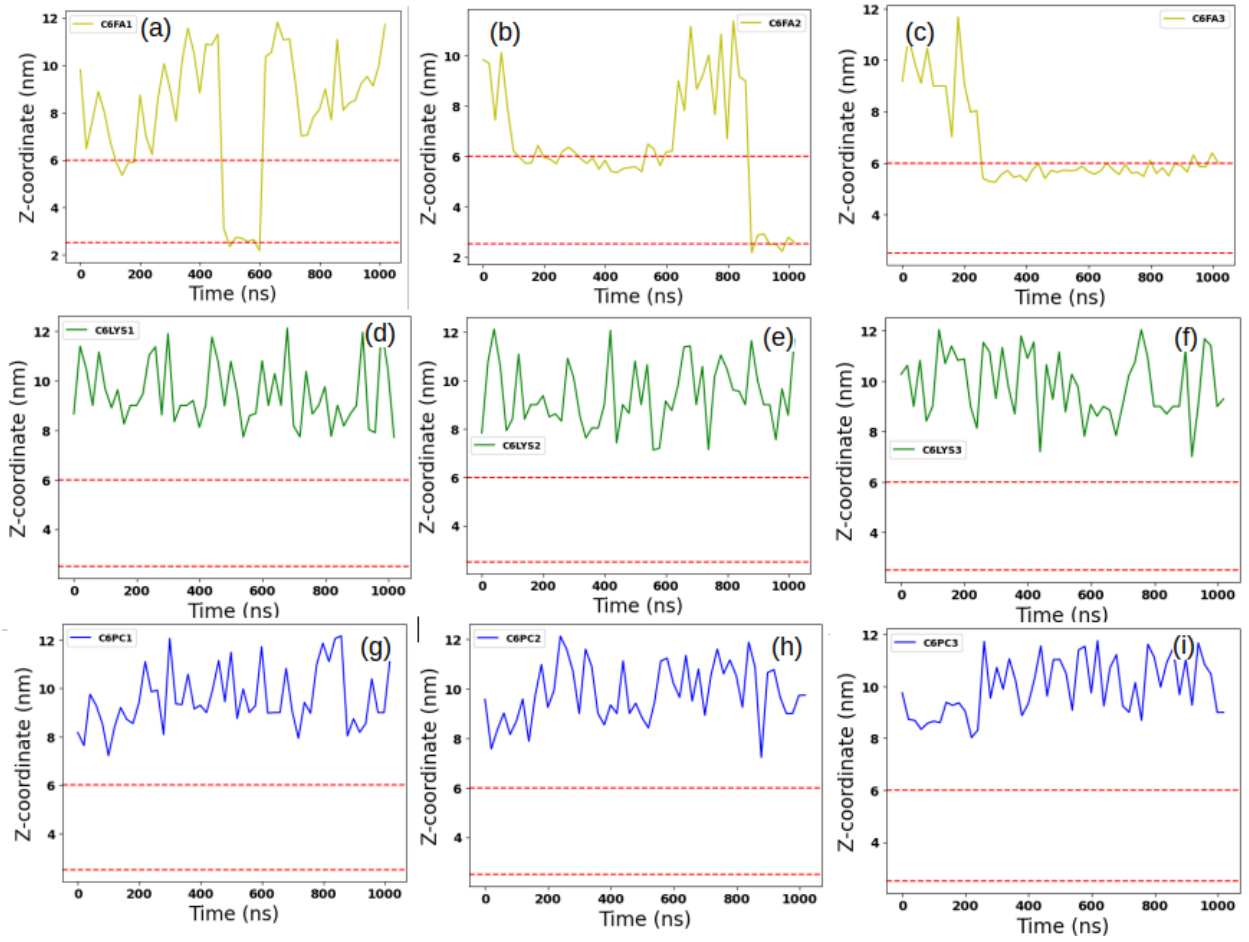

Figure S11: Z-coordinate of different molecules in DPPC-CHOL membrane system profiles over time ((a-c)C6FA, (d-f) C6LYS, (h-i) C6PC and the number followed after the molecule names indicate the index for different molecules. The red dashed lines represent the upper and lower limits of the bilayers.

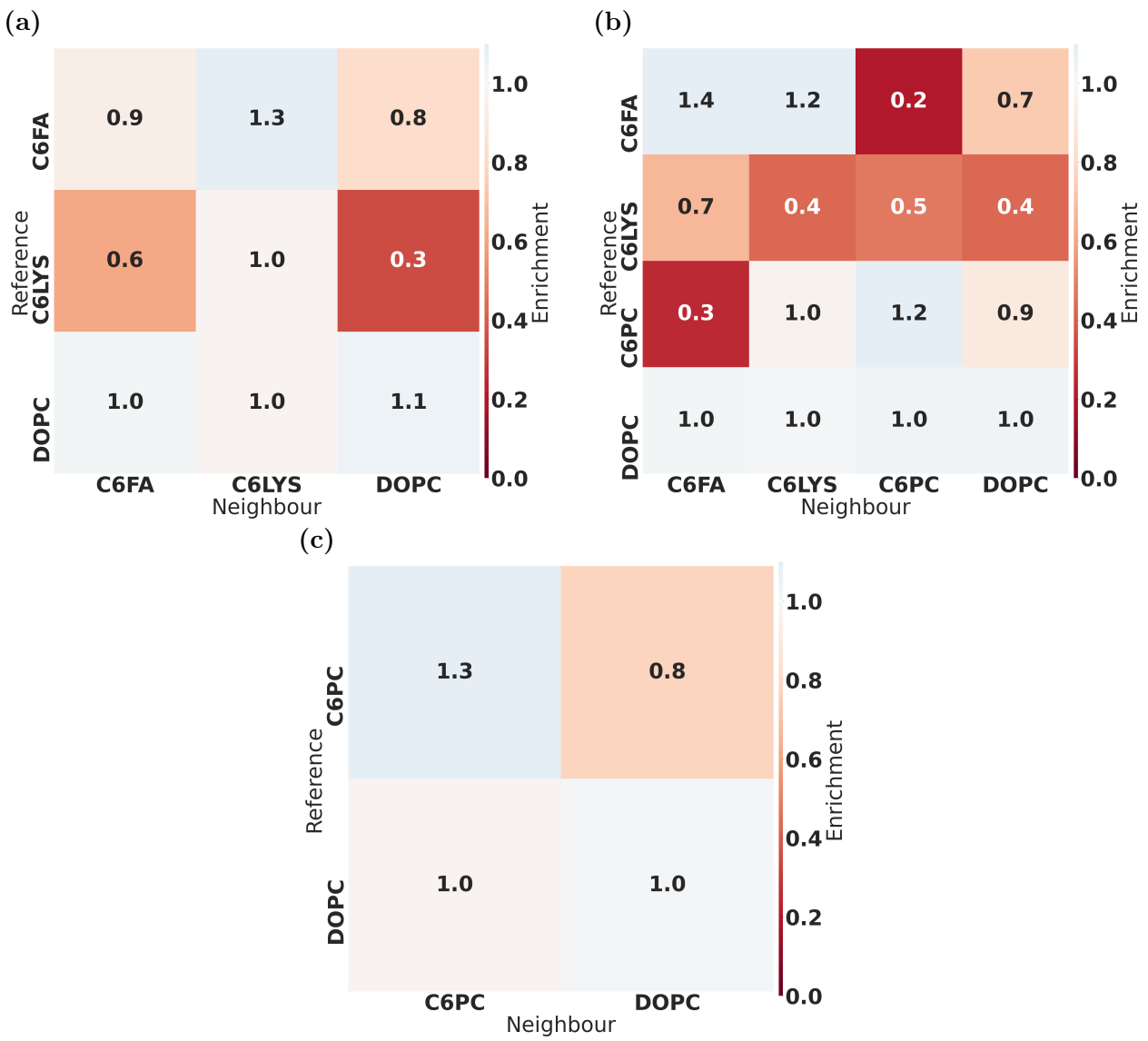

Figure S12: Enrichment/ Depletion index for DOPC-Pure-Products (a), DOPC-Mixed (b), DOPC-Pure-Lipids (c) membrane systems, calculated using the last 200 ns of each simulation. Values above and below 1 indicate enrichment and depletion, respectively.

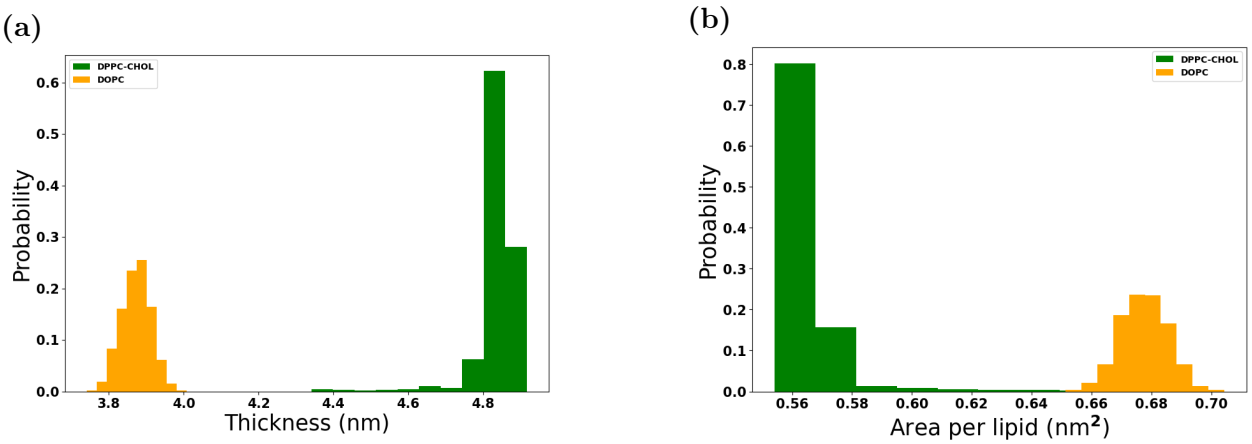

Figure S13: Membrane thickness (a) and area per lipid (b) as function of time in pure membrane systems.

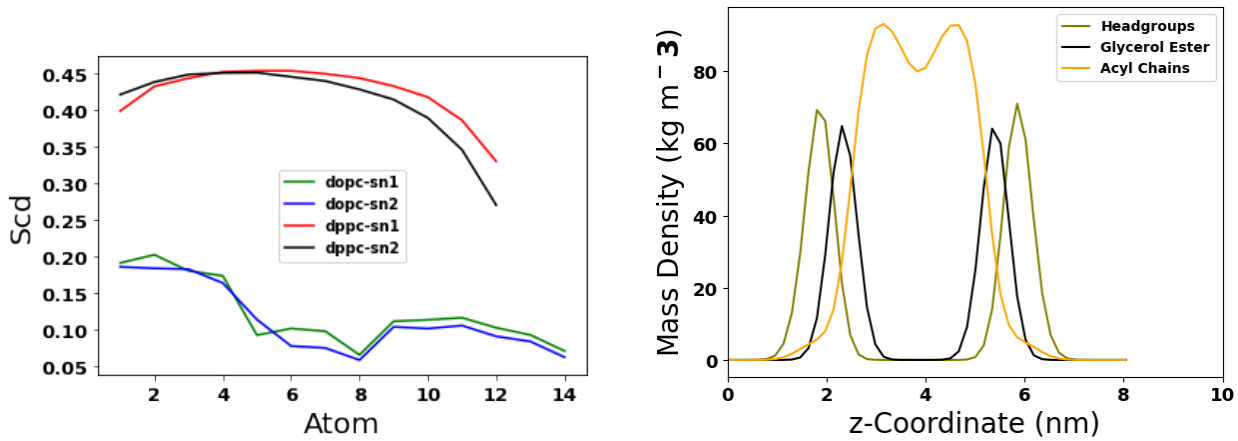

(a) order parameters **(b) mass density profile for DOPC**

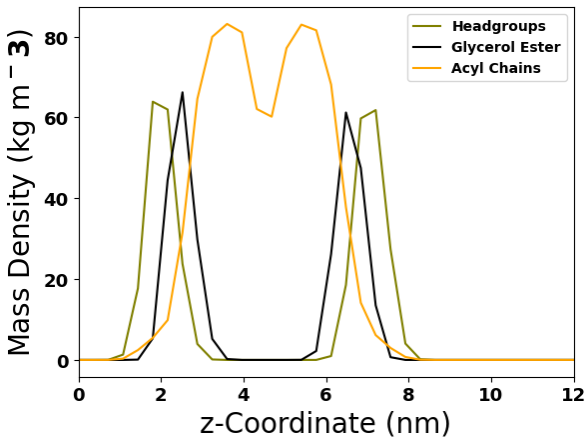

(c) mass density profile for DPPC-CHOL

Figure S14: The absolute values of (a) the lipid order parameters and mass density for the pure (b) DOPC and (c) DPPC-CHOL membranes.

Properties of Pure Membrane

Different phases of pure lipid membranes have been studied by various simulation and experimental methods.[1–3] In our study, we have measured several properties including the membrane thickness, the area per lipid and the lipid tail order parameter, to capture the differences in these two pure membrane systems and get them visualized shown in Figure S3. During the 200 ns simulation performed for the two membranes, the thickness of the DOPC system (Figure. S13(a)) fluctuates from 3.8 nm to 4.0 nm (the average value is 3.9 nm and the standard deviation is 0.04) whereas there is a increasing trend for DPPC-CHOL up to 4.87 nm. When it comes to the area per lipid, we find again that the value is more or less constant around 0.68 nm^2 (the average value is 0.68 nm^2 in DOPC membrane system (Figure. S13(b)) whereas in the DPPC-CHOL system We find that the area per lipid decreases over the first 25 ns and then reaches an approximate value of 0.57 nm^2 (the average value is 0.57 nm^2 and the standard deviation is 0.01 over the last 100 ns) . The fact that for the DPPC-CHOL membrane we have found a larger membrane thickness and a smaller area per lipid is in agreement with previous studies of similar systems which show these effects as a result of the condensing effect of cholesterol in membranes.[4–6] These results indicate that these two lipid membranes represent two distinct phases, liquid-disordered (DOPC) and liquid-ordered (DPPC-CHOL) phases. They are also in agreement with other studies that a decreased membrane thickness is normally accompanied by an increase in area per lipid.[7]

The profiles of the deuterium order parameter for DOPC and DPPC-CHOL membrane systems are shown in Figure S14(a) . The surface area of the lipids is normally inversely related to the deuterium order parameter. A more compact bilayer usually has a higher deuterium order parameter and vice versa.[8] We see that the value of order parameters for DPPC-CHOL is much larger than those for DOPC, which means the DPPC-CHOL systems are rigid in comparison with pure DOPC membrane and this trend is in agreement with the previously studied by Verde et al.[9,10] As the tails of each DOPC have two-double bonds and longer than DPPC (have two more carbon atoms), it also makes the structure of membrane

less stable and more fluid so the twisted lines can be observed as well. It has been proposed that the single bonds next to the double bond can rotate relatively easily.[11] The lowest point in DOPC membrane system (the green and blue lines) are located in the 8^{th} carbon where the position of double bond atom is and it makes it unstable. Comparing to the DPPC-CHOL membrane system (the red and black lines), each line for tails sn1 sn2 are more smooth and it means the structure of lipid changed less.

By computing mass density profiles for these two different pure membrane systems showed in Figure S14 (b) DOPC and (c) DPPC-CHOL, we can also determine the approximate positions of upper leaflet and lower leaflet with z-coordinate of headgroups on each system.

References

(1) Nagle, J. F.; Tristram-Nagle, S. Structure of lipid bilayers. *Biochim. Biophys. Acta Biomembr.* **2000**, *1469*, 159–195.

(2) Prates Ramalho, J.; Gkeka, P.; Sarkisov, L. Structure and phase transformations of DPPC lipid bilayers in the presence of nanoparticles: insights from coarse-grained molecular dynamics simulations. *Langmuir* **2011**, *27*, 3723–3730.

(3) Hakobyan, D.; Heuer, A. Phase separation in a lipid/cholesterol system: comparison of coarse-grained and united-atom simulations. *J. Phys. Chem. B* **2013**, *117*, 3841–3851.

(4) Loura, L. M.; do Canto, A. M. M.; Martins, J. Sensing hydration and behavior of pyrene in POPC and POPC/cholesterol bilayers: A molecular dynamics study. *Biochim. Biophys. Acta Biomembr.* **2013**, *1828*, 1094–1101.

(5) Shahane, G.; Ding, W.; Palaiokostas, M.; Orsi, M. Physical properties of model biological lipid bilayers: insights from all-atom molecular dynamics simulations. *J. Mol. Model.* **2019**, *25*, 1–13.

(6) Róg, T.; Pasenkiewicz-Gierula, M.; Vattulainen, I.; Karttunen, M. Ordering effects of cholesterol and its analogues. *Biochim. Biophys. Acta Biomembr.* **2009**, *1788*, 97–121.

(7) Tristram-Nagle, S.; Petrache, H. I.; Nagle, J. F. Structure and interactions of fully hydrated dioleoylphosphatidylcholine bilayers. *Biophys. J.* **1998**, *75*, 917–925.

(8) Douliez, J.-P.; Leonard, A.; Dufourc, E. J. Restatement of order parameters in biomembranes: calculation of CC bond order parameters from CD quadrupolar splittings. *Biophys. J.* **1995**, *68*, 1727–1739.

(9) Bonn, M.; Roke, S.; Berg, O.; Juurlink, L. B.; Stamouli, A.; Müller, M. A molecular view of cholesterol-induced condensation in a lipid monolayer. *The Journal of Physical Chemistry B* **2004**, *108*, 19083–19085.

(10) Leekumjorn, S.; Wu, Y.; Sum, A. K.; Chan, C. Experimental and computational studies investigating trehalose protection of HepG2 cells from palmitate-induced toxicity. *Biophys. J.* **2008**, *94*, 2869–2883.

(11) Kulig, W.; Pasenkiewicz-Gierula, M.; Róg, T. Cis and trans unsaturated phosphatidylcholine bilayers: a molecular dynamics simulation study. *Chem. Phys. Lipids* **2016**, *195*, 12–20.